Measurements of the anatomical distribution of erythemal ultraviolet: a study comparing exposure distribution to the site incidence of solar keratoses, basal cell carcinoma and squamous cell carcinoma

Nathan Downs[1] and Alfio Parisi[1]

[1] Faculty of Sciences, University of Southern Queensland, Toowoomba, 4350, Australia.
email downsn@usq.edu.au, Fax: +617 46 312721, Tel: +617 46312727

Abstract

Measurements of anatomical UV exposure distribution were made using miniaturized polysulphone dosimeters over a four year period between 2005 and 2008 in Toowoomba, Australia (28^{o}S, 152^{o}E). Anatomical UV exposures were expressed relative to the horizontal plane ambient UV. The UV exposures were compared with existing data detailing the anatomical distribution of basal cell carcinoma (BCC), squamous cell carcinoma (SCC) and Solar keratoses (SK). Surface UV exposures to unprotected skin surfaces have been presented for each of the face, neck, arm, hand and leg assessing a total of 1453 body sites (2491 measurements). Measured exposures are presented for the human facial region to a resolution of 5 mm. The median anatomical UV, expressed relative to the horizontal plane ambient UV for each of the face, neck, forearm, hand and leg regions of the body varied from 26%, 23%, 13%, 30% and 12% respectively in the 0^{o}-30^{o} SZA range; 39%, 36%, 17%, 35% and 23% in the 30^{o}-50^{o} SZA range; and 48%, 59%, 41%, 42% and 47% in the 50^{o}-80^{o} SZA range. Detailed positions of UV exposure measured over the face, neck, arm, hand and leg were more closely related to NMSC incidence data for the face and upper limbs. Further analysis with existing facial BCC and SK density data did not however show a direct relationship with the measured UV exposures highlighting the importance of other factors influencing the causation and localisation of facial NMSC.

Keywords: Ultraviolet, erythema, non-melanoma skin cancer, polysulphone dosimetry.

Introduction

Non melanoma skin cancer (NMSC) is the most common type of cancer observed in fair skinned populations[1]. Of the types of NMSC, basal cell carcinoma (BCC) occurs more frequently, originating in the basal cell layer of the epidermis varying in depth from between 40 μm for the head, 50 μm for the arms and legs and 150 μm for the dorsal sides of the hand[2]. Squamous cell carcinoma (SCC), affecting the stratified squamous epithelium occur frequently to exposed areas of human skin. The incidence of SCC and BCC increases with age[3,4] and is strongly correlated in fair skinned populations living in low latitudes. Exposure to ultraviolet (UV) radiation plays a causative role in the gene mutation of skin carcinomas[5], penetrating the dermal layer over the UVA waveband, reaching subcutaneous tissue[6] and affecting the epidermal layer in both the UVA and UVB wavebands. The ambient UV incident upon skin surfaces of the human body is strongly dependent on geographical latitude, having a significantly greater intensity in lower latitudes due to higher solar elevation. Low geographical latitude and the predominately northern European ethnocentric origin of the modern Australian population contribute to Australia having the largest incidence rates of NMSC in the world, displaying a distinct latitudinal gradient[7].

Like NMSC, actinic or solar keratoses (SK) are also commonly observed in fair skinned populations that are exposed to high ambient levels of UV radiation such as those which occur in Australia[8,9]. These cutaneous legions have been noted to be more prevalent on sun exposed regions of the body compared to BCC and SCC leading to SK being noted as potentially better markers of sunlight exposure than the presence of skin cancers[8]. In addition to SK forming in frequently sun exposed regions of the body, SCC have been linked to the presence of pre-existing SK legions[10] leading to their being recognised as either pre-cursors to, or representative of the developmental stages of SCC[11]. In this research, the published facial distribution of SK[12]incidence and BCC[13] incidence was compared to measured facial site UV exposure data in the 0^o-30^o, 30^o-50^o and 50^o-80^o solar zenith angle (SZA) ranges. This extends the work of previous research which has published NMSC site incidence data over broader regions of the body and face.

In 1979, Diffey[13] published measurements of UV exposure made at 40 facial locations on a large fiberglass headform. These results were shown in comparison to detailed published BCC facial site incidence data[14]. Unlike the study of Diffey[13] which utilised a mannequin headform, studies of sun exposure measured to individuals have not been able to accurately link measured exposures to the development of skin cancers due to the limited number of body sites that can be assessed on living human subjects and the extended latency period

between an exposure event and the development of a cancer. Furthermore, whilst the distribution of NMSC to the human body has been extensively documented including studies conducted by Peal and Scott[15], Kricker et al.[16] and Raasch[17], detailed NMSC site distributions are often limited to broad regions of the body making direct comparisons between body surface exposure and NMSC site incidence difficult.

The pattern in UV exposure received by specific body sites, being dependent upon SZA is critical toward understanding frequency of incidence and anatomical distribution of NMSC present in worldwide populations. The current study provides results on the UV exposure distribution received by surfaces of the human body with variation in SZA to a spatial resolution of between 5 mm and 20 mm to the face, neck, forearm, hand and leg. This research extends previously detailed measurements of exposure recorded on the face over three SZA ranges[18], where preliminary results were provided for a number of facial sites. These earlier results for UV exposures over the human facial topography are extended in this paper to provide detailed measurements of facial and body surface UV exposures made under low and high cloud cover conditions. Measurements of UV surface exposures are further compared with facial and body site NMSC and SK incidence data.

Methods

Exposure Ratio

Measurements of ultraviolet exposure were made using miniaturized polysulphone dosimeters. The miniaturized dosimeters used in this research were chosen to be small and flexible enough to be attached in large numbers to the complex surface topography of a life sized mannequin model. Each miniaturized dosimeter was made using a flexible card frame measuring approximately 10 mm by 15 mm with a clear circular aperture of 6 mm over which polysulphone film of an approximate thickness of 40 μm was adhered. Pre- and post-exposure measurements of polysulphone film absorbance were made at 330 nm using a spectrophotometer (model 1601, Shimadzu Co., Kyoto, Japan) and subsequent exposures were expressed relative to the horizontal plane exposure measured in proximity to the mannequin. Here, the exposure measured at any site and expressed relative to the horizontal plane exposure is given by:

$$ER = \frac{E_{site}}{E_{hor}} \qquad (1)$$

where *ER* is the exposure ratio of the UV exposure measured at any given body site, E_{site}, and expressed relative to the horizontal plane exposure, E_{hor}. Both E_{site} and E_{hor} are the erythemal UV exposures measured with the dosimeters for the exposure periods listed in Table 1 within the SZA ranges 0^o-30^o, 30^o-50^o and 50^o-80^o. For the SZA range 0^o-30^o, measurements were made between November and March near solar noon, and varied for the SZA ranges 30^o-50^o and 50^o-80^o depending on the calculated SZA position for the months April to October. The ER was chosen as a valuable method of representing exposure to body surfaces relative to the horizontal plane ambient as measurements from several experiments could be combined with reasonable certainty. The erythemally effective exposures, *E* were calculated using the representation[19]:

$$E = K(9\Delta A^3 + \Delta A^2 + \Delta A) \qquad (2)$$

For which, ΔA is the change in polysulphone film absorbance measured at 330 nm and *K* is a constant that is eliminated in the ratio, *ER*. The estimated uncertainty of the miniaturized dosimeters due to variation in ΔA was determined for this research to be ± 7% (1 σ). Uncertainty in the measured exposure ratio, *ER* is therefore taken to be in the order of 14% for all measurements quoted here.

Measurement sites

Measurements of ER were taken at up to 1453 body sites on the mannequin face (709 sites), neck (98 sites), forearm (166 sites), hand (247 sites) and leg (233 sites). Sites on each of the five body parts were organized into horizontal and vertical contours. Contours on the face and hand were separated by 5 mm, 10 mm on the arm and neck, and 20 mm on the leg. Vertical and horizontal contours were drawn onto each body part. The intersection of each vertical and horizontal contour was also marked on the mannequin models and used as a viable dosimeter location. Two mannequin models were used to measure the UV exposure to each of the body parts. These included a headform which was used to represent facial and neck ER distribution, and a whole body mannequin which was used to represent arm, hand, and leg ER. ER data measured at each contour intersection site was plotted onto three dimensional contour representations of each body part. This technique, used previously[18], colours the three dimensional contour wireframe model of each mannequin body part depending on the ER of each individual body part subsite which represent individual measured mannequin contour intersections or viable dosimeter locations. The data presented as a colour wireframe mesh has also been provided in tabular form in the supplementary material and was organized into tables for each of the face, neck, arm, hand and leg, listing actual measurements of UV

exposure relative to the horizontal plane ambient UV. Data presented in tables represent all of the ER data collected in the 2005 to 2008 measurement period. Where no data is listed no measurements have yet been taken for that subsite location. A Total of 2491 ER subsite measurements were taken in the 2005 to 2008 measurement period. ER measurement dates, SZA range, body part and cloud coverage for each exposure period are listed in Table 1. Exposure times were limited to the SZA ranges given in the table for each experiment. Typical exposure periods were 2 hours in duration.

Table 1. Date, SZA ranges and cloud cover experienced during mannequin body measurements conducted in the period 2005 through to 2008.

Mannequin Measurement Location

Face			Neck			Arm			Hand			Leg		
Date	SZA (°)	cloud (okta)	Date	SZA (°)	cloud (okta)	Date	SZA (°)	cloud (okta)	Date	SZA (°)	cloud (okta)	Date	SZA (°)	cloud (okta)
18 Feb 06	0-30	4	14 Nov 07	0-30	1-3	13 Dec 07	0-30	5-7	21 Nov 07	0-30	2-3	13 Nov 07	0-30	2
12 Mar 07	0-30	1	25 Jan 08	0-30	2-5	01 Feb 08	0-30	3-5	01 Feb 08	0-30	3-5	01 Feb 08	0-30	3-5
21 Feb 08	0-30	2-4	18 Dec 07	30-50	7-8	30 Apr 07	30-50	0	02 Apr 08	30-50	1-2	04 Mar 08	30-50	3-2
25 Jan 08	0-30	2-5	27 Aug 07	50-80	1	02 Apr 08	30-50	1-2	28 Aug 07	50-80	4-5	06 Aug 07	50-80	0
14 Nov 07	0-30	1-3				18 Jul 07	50-80	0				02 Aug 08	50-80	0
16 Sep 05	30-50	0				12 Jul 07	50-80	0						
5 Oct 06	30-50	3												
16 Oct 07	30-50	0												
16 Oct 07	50-80	0												
27 May 05	50-80	0												
27 Aug 07	50-80	0												

For the ER data presented in the supplementary tables, each column was taken to represent a vertical contour on each mannequin body part including vertical contours that passed from the forehead through to the front of the neck for the face model; the base of the skull to the lower back of the neck for the neck model; the shoulder to the wrist for the arm model, the wrist to the finger tips for the hand model, and the upper thigh to the ankle for the leg model. Horizontal contours were represented as rows in each body part table and extended from the centre of the face toward the ear for the face model; from the centre of the back of the neck to the side of the neck for the neck model; and complete connected bands for the arm, hand and leg models whereby the first horizontal contour represents a band located at the shoulder for the arm; a complete band around the wrist for the hand model and a complete thigh band for the leg model. Where more than one measurement has been recorded at a specific body part subsite, mean ER is listed for that site location for the supplementary tables presented in this research. ER measurements presented in the tables are the collected ER measured within each SZA range and may therefore have been measured on different days under different atmospheric conditions (Table 1). Uncertainties in ER were minimized by representing body site exposure relative to the horizontal plane ambient UV. The data has been shown

collectively for the four year measurement period to minimize the number of exposure tables that need to be presented in this work. Supplementary figures of the ER for each body part in the SZA ranges 0^o-30^o, 30^o-50^o and 50^o-80^o were constructed from tabular representations of mean body site ER recorded in the 2005 to 2008 measurement period.

Both mannequins used in this study were placed on a rotating platform that completed approximately two revolutions per minute. The rotating platform and mannequins were placed in open environments which were located at least 30 m from the nearest buildings inside the grounds of the University of Southern Queensland Toowoomba campus (28^oS, 152^oE). Measurements of the ER were made over a four year period between 2005 and 2008. The measurement intervals were taken under low cloud cover conditions where possible during periods when the SZA varied from 0^o-30^o, 30^o-50^o and 50^o-80^o.

Incidence data

For this research, NMSC incidence data from two Australian studies were compared to the median ER measured to the face, neck, arm, hand and leg mannequin models. Both of these studies detailed BCC and SCC incidence rates based on either clinical or histological diagnosis of either NMSC in their respective study populations. Body site incidence data for both BCC and SCC were detailed for the face, neck, leg and upper limbs where the upper limb groups included lesions diagnosed to the arms and hands together. Both study groups presented NMSC incidence data collected in similar latitudes to the measured UV exposure distributions presented in this research.

Detailed facial site UV exposures measured in this study were further compared to histologically confirmed BCC incidences recorded by Brodkin[14] as detailed by the exposure comparison of Diffey et al.[13]. This data set, excluding superficial type BCC were diagnosed in the Oncology Section of the Skin and Cancer Unit, University Hospital, New York, and may therefore differ in BCC distribution observed in an Australian population for which the ambient UV environment is likely to be different to that which subjects diagnosed in the Brodkin et al.[14] study were exposed. This data set was however sufficiently detailed to make a comparison to the current UV distribution exposure sets allowing for a comparison of 39 facial locations illustrated in the study conducted by Diffey et al.[13]. The facial SK incidence data compared in this study was sourced from published naevi and SK facial distributions[12]. Published SK data detailed in the Nguyen et al.[12] study data was comprised of 79 adult participants taking part in a field trial located in the Nambour region of Southern Queensland[20]. These participants were diagnosed by a medically qualified investigator as

having at least one SK located on the head or neck. The Nambour region is located within approximately 200 km of the Toowoomba measurement site.

Results

Patterns in facial exposure

The face is not regularly protected by clothing as are other regions of the body that are exposed to the ultraviolet environment. Correspondingly, non melanoma skin cancers are highly prevalent on the face followed by other regions of the body that receive high solar UV exposures including the arms, hands and legs[15,16,17]. Within the human facial region, the nose, ears and cheeks receive the highest proportions of ambient UV[13,21]. Of these facial regions, the nose often receives the greatest proportion of ambient UV over a large SZA range[22,23,18]. Supplementary tables 1(a), 1(b) and 1(c) list the erythemally effective ER measured to the face under low cloud cover conditions for SZA ranges of 0^o-30^o, 30^o-50^o and 50^o-80^o respectively. The tables are organized into 18 vertical and 49 horizontal contours. A clear increase of the exposure relative to the horizontal plane toward the lower proximities and outer extremities of the face is evident in the data for lower solar elevations (larger SZA).

Patterns in body surface exposure

Table 2 represents the variation in measured ER for each of the body parts studied in this research. The minimum, maximum, median and first and third interquartile ranges are listed in the table. The highest measured exposure relative to the horizontal plane UV was received by the face at the vertex in each SZA range. Of each of the face, neck, arm, hand and leg body parts studied in the 0^o-30^o SZA range, the dorsum of the hand received the highest exposure relative to the horizontal plane UV, followed by the face, the back of the neck, the forearm and legs.

Table 2. Exposure ratio statistics, expressed as a percentage of the horizontal plane ambient UV and listed for the face, back of the neck, forearm, hand and leg in the SZA ranges 0^o-30^o, 30^o-50^o and 50^o-80^o.

	Face		
	0^o-30^o	30^o-50^o	50^o-80^o
Range	1-100%	6-100%	0-100%
IQR	15-47%	24-58%	33-70%
Median	26%	39%	48%
Total measurements	391	154	229
	Neck		
	0^o-30^o	30^o-50^o	50^o-80^o
Range	4-67%	13-69%	19-86%
IQR	16-33%	30-44%	49-67%
Median	23%	36%	59%
Total measurements	170	44	23
	Forearm		
	0^o-30^o	30^o-50^o	50^o-80^o
Range	3-61%	0-55%	2-88%
IQR	5-29%	7-35%	21-57%
Median	13%	17%	41%
Total measurements	140	175	109
	Hand		
	0^o-30^o	30^o-50^o	50^o-80^o
Range	1-76%	1-76%	0-84%
IQR	8-51%	12-57%	10-61%
Median	30%	35%	42%
Total measurements	264	119	82
	Leg		
	0^o-30^o	30^o-50^o	50^o-80^o
Range	1-39%	4-52%	12-82%
IQR	9-16%	15-33%	37-57%
Median	12%	23%	47%
Total measurements	248	231	112

Exposures measured within the 0^o-30^o SZA range received the strongest UV irradiance. This is due to high solar elevation and reduced atmospheric absorption caused by incident sunlight moving through a shorter atmospheric path than occurs at greater SZA. The measured pattern of exposure would commonly be observed in sub-tropical to low latitudes during the summer months either side of midday. At greater SZA ranges, the face and neck receive the highest ER for the 30^o-50^o and 50^o-80^o SZA ranges with the hand and leg receiving higher exposures than the forearm. This is due to UV radiation incident in the greater SZA ranges having a more significant influence on vertically orientated body surfaces.

Exposures to all body parts measured in this study showed an increase in ER with increasing SZA range. Apart from the ER measured in the 0^o-30^o SZA range for the back of the neck, all body parts showed a further increase in the interquartile range of exposures. These findings

indicate that the UV exposure received over the body surface increases relative to the horizontal plane exposure and affects a larger surface area of the body with increasing SZA.

While there is a clear spreading in the received exposure over a larger area with increasing SZA, exposures measured in the high SZA ranges were received during periods of the day that receive a lower UV irradiance. The lower ER measured at sites in the 0^o-30^o SZA range receive a significant level of the ambient UV due to the higher UV irradiances at these smaller SZA. The measured ranges of exposure listed in Table 2 therefore provide an indication of the proportions of each body part at risk of receiving high levels of solar UV radiation. For populations located in sub-tropical to low latitudes that experience high solar elevations, and subsequently all of the SZA ranges studied in this research, the areas of the body surface that receive the highest UV exposure are those highlighted in the 0^o-30^o SZA range. The areas of the body that receive the highest UV exposure based on a comparison between all studied SZA range distributions are therefore the vertex, the nose, the cheeks, the top of the ear, the dorsa of the forearms and hand, the lower back of the neck located near the shoulder, and the calf muscle region of the leg.

Comparison of measured exposure with sites of NMSC incidence

The anatomical distribution for histologically confirmed incidences of BCC and SCC measured in Australian populations of sub-tropical and tropical latitude were compared to the ER data measured in the 0^o-30^o, 30^o-50^o and 50^o-80^o SZA range. The localisation of BCC and SCC data were measured from electoral roll populations residing in Geraldton, Western Australia[16] and Townsville, Queensland[17]. These two regional Australian cities are located in latitudes of 29^oS and 19^oS respectively and are therefore subject to the SZA ranges studied in this research. The incidence of both BCC and SCC to the face and upper limbs were reported in these two studies to be higher than the confirmed incidences to the neck and legs, regions of the body that are better protected by clothing than the face and upper limbs, particularly in warm climates, where often the forearms are not protected.

Generally, BCC incidence reported by Kricker et al.[16] and Raasch et al.[17] was most strongly correlated to UV exposures measured in this research to the face, followed by the upper limbs. Both of these studies further reported the greatest incidence of BCC to the legs followed by the neck, however exposures measured in this research were higher to the neck region followed by measurements made to the legs of the mannequin. The examined incidences of SCC which were recorded in similar latitudes to the measured pattern of exposure show a higher correlation with ER than the respective BCC incidence where the facial incidence of this cancer was greater than the incidence to the upper limbs in the

Geraldton[16] study and lower in the Townsville[17] study. Here the facial incidence of SCC was measured in Geraldton[16] to be 58% and 57% (men and women respectively) and 19% in Townsville[17] and the incidence to the upper limbs was measured at 9% and 14% (men and women) in Geladton[16] and 49% in Townsville[17] essentially demonstrating that approximately half of the observed SCCs occurred to frequently exposed regions of the body. The patterns in solar UV exposure affecting unprotected skin surfaces measured in this research may therefore be found to be in better agreement with future studies relating the anatomical distribution of SCC than BCC. A more detailed analysis of measured ER and subsite incidence rates is however needed to determine associations between exposure and whole body incidence of NMSC.

Comparisons with facial BCC and SK site incidence to UV exposure

Comparison between the facial distribution of UV exposure and the localisation of BCC incidence has been reported previously[13]. The facial distribution of BCC incidence has been detailed by Brodkin et al.[14], Scrivener et al.[24] and more recently by Richmond-Sinclair et al.[25] in and Australian setting. These studies show high rates of BCC incidence to the nose. Comparisons between the distribution of facial exposure and BCC incidence provide a valuable insight into the causal nature of UV exposure and the aetiology of BCC as the face is not often protected by clothing and receives a high proportion of the ambient UV. The correlation between facial BCC tumour density[14] and UV exposure examined by Diffey et al.[13] did not show a strong relationship. This was partly due to differences in latitude between the two locations in which the data sets were collected. The facial UV exposure data recorded in the current study within each of the 0^o-30^o, 30^o-50^o and 50^o-80^o SZA ranges is presented in figure 1. Comparisons made between the research of Diffey et al.[13] and the current facial exposure measurements show similarities that highlight the difficulty in establishing a relationship between UV exposure and BCC tumour density. The data presented shows a steady increase in BCC tumour density with increasing UV exposure ratio, however consistent discontinuities in the comparison weaken the relationship with significantly higher tumour densities occurring for example, under the nose, an area of the face that does not receive a high proportion of the ambient UV.

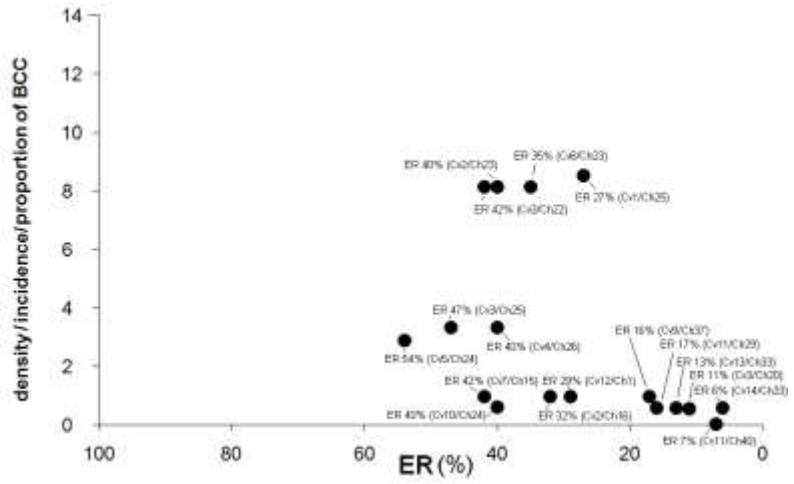

Figure 1(a) Facial BCC tumour incidence[14] and UV exposure in the SZA 0°-30°.

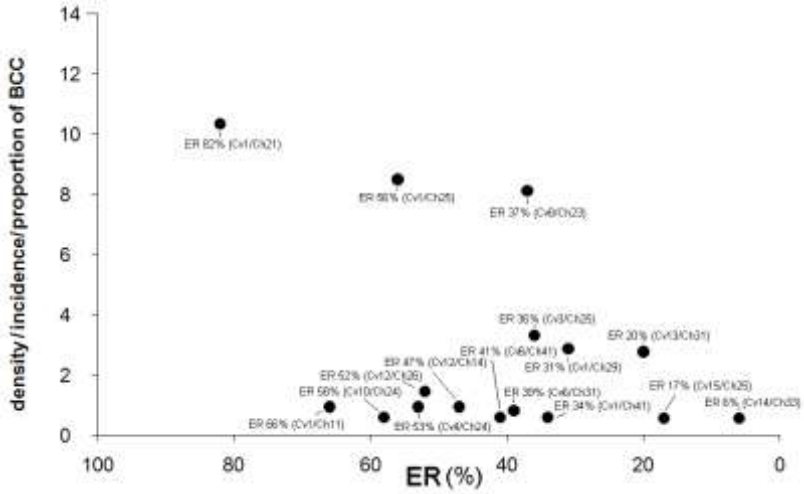

Figure 1(b) Facial BCC tumour incidence[14] and UV exposure in the SZA 30°-50°.

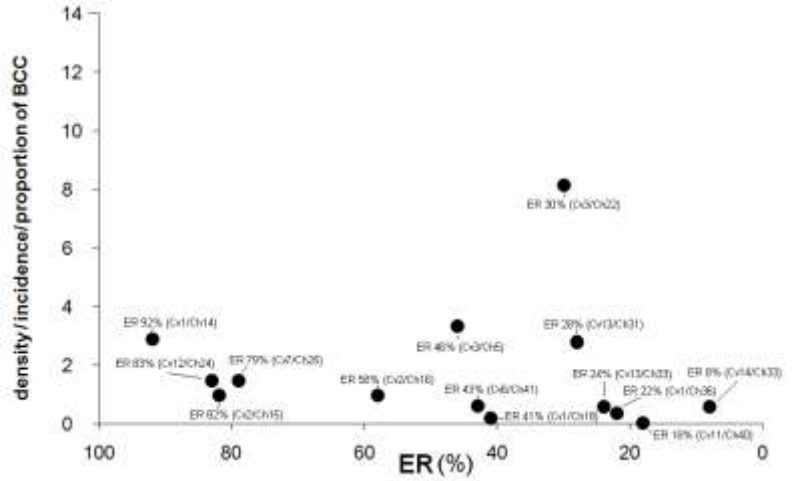

Figure 1(c) Facial BCC tumour incidence[14] and UV exposure in the SZA 50°-80°.

The relationship between facial UV exposure and the distribution of SK, possible markers for the later development of SCC[8], were examined with respect to measured facial ER. Figure 2 compares the facial distribution of SK incidence measured in Nambour (Latitude 27° S)[12] with the facial ER data measured here for each of the 0°-30°, 30°-50° and 50°-80° SZA ranges. Comparisons between this data set show that SK incidence increases with facial UV exposure. The greatest incidence of observed SK for the Nambour study[12] was found on the cheek, followed by the ears and the nose. Each of these regions of the face receive a consistently high UV exposure across each of the 0°-30°, 30°-50° and 50°-80° SZA ranges. However, as is evident in figure 2, it is difficult to establish a clear relationship between UV exposure distribution and the incidence of SK.

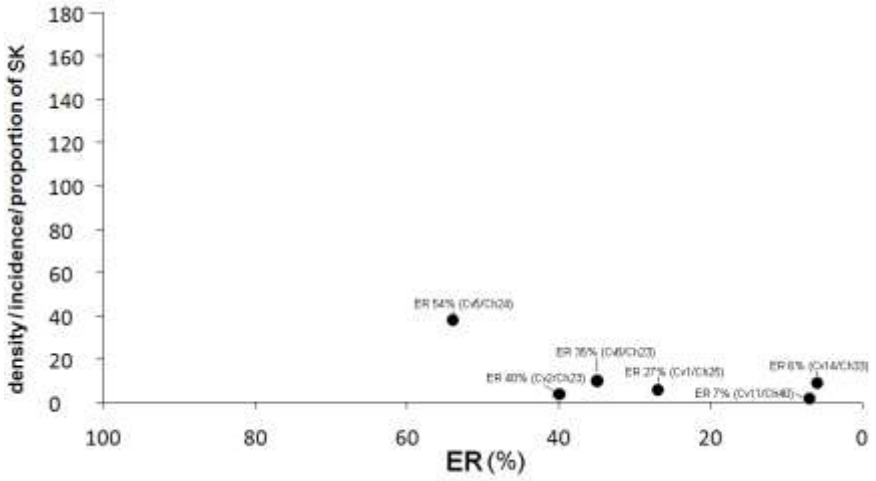

Figure 2(a) Facial SK incidence[12] and UV exposure in the SZA 0°-30°.

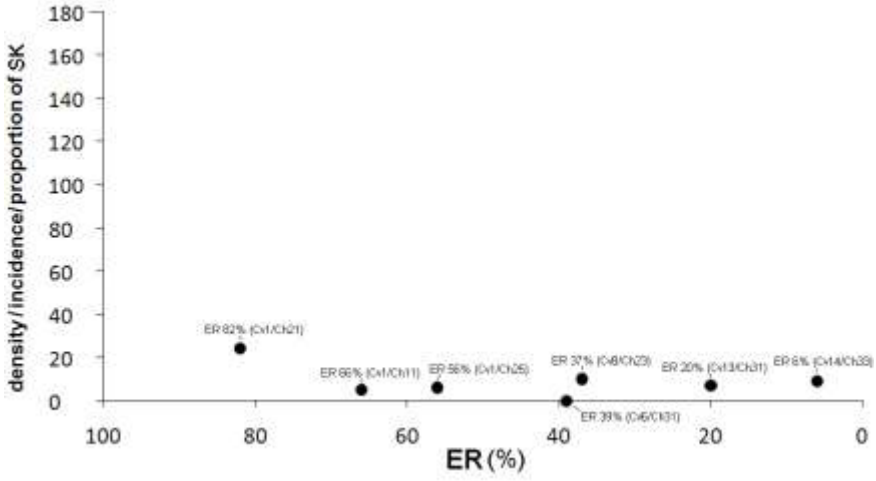

Figure 2(b) Facial SK incidence[12] and UV exposure in the SZA 30°-50°.

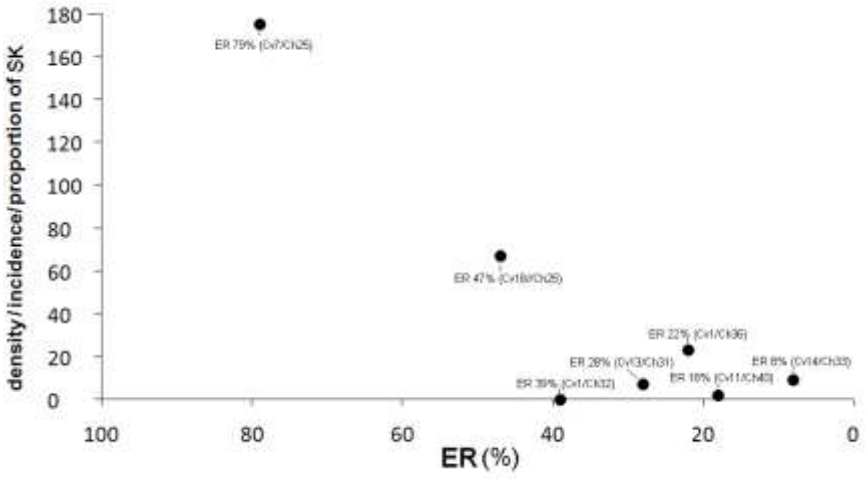

Figure 2(c) Facial SK incidence[12] and UV exposure in the SZA 50^{o}-80^{o}.

Discussion

This research has presented detailed subsite information for facial exposures in the 0^{o}-30^{o}, 30^{o}-50^{o} and 50^{o}-80^{o} SZA ranges. Measurements of exposure were consistently high over the scalp region of the facial mannequin model in each SZA range. Periorbital exposures tended to be low across all SZA ranges although greater exposures were observed over the upper cheek region with increasing SZA. Summary statistics were given for neck, arm, hand and leg body models. It was determined that higher exposure occurred on body parts orientated more closely toward the horizontal plane. These included the lower back of the neck toward the shoulder region, the lower anterior of the forearm, the dorsa of the hand and the upper anterior calf muscle region of the leg. Each of these subsites received a higher proportion of the ambient UV with increasing SZA.

The incidence of SCC in men and women is lower than BCC[7,16,17]. The proportion of SCC is greater to the exposed surfaces of the upper limbs than BCC[17,26]. This, in part is due to the higher incidence rate of BCC localised on the body trunk, an area of the body not readily exposed to solar UV, decreasing the relative proportion of BCC incidence to frequently exposed body surfaces. Patterns in BCC incidence supported by the hypothesis that intermittent exposures affect areas of the body not readily exposed to solar UV, may account for BCC anatomical distributions that develop later in life as a result of earlier severe episodes of sunburn. Chronic exposure to solar UV is more likely to establish a pattern in exposure similar to that which has been measured in this research as it can reasonably be concluded

that chronic exposure to solar UV will affect unprotected skin surfaces of the body that receive a higher solar UV exposure.

Nevertheless, the aetiological factors that influence the development of NMSC cannot be directly related to the measured anatomical distribution of UV exposure alone. The relevance of this particular point must be emphasised in relation to the currently presented erythemal UV exposure distributions which were measured using upright mannequin subjects. The current research cannot therefore account for situations including sunbathing or indeed all of the exposure situations likely to be experienced within an individual's lifetime. Additional factors including variation in skin thickness above the basal layer, the presence of hair, clothing, and personal outdoor lifestyle patterns will influence NMSC incidence rates and are difficult to quantify with respect to comparisons made using mannequin subjects.

Existing data present in the literature detailing the measured distribution of solar UV exposure to human subjects is limited by the total number of body sites that can be measured. An approach that integrates detailed measurements of UV exposure distribution, such as the body exposure sets provided here may improve interpolated estimates of whole body exposure measured using human subjects which in turn may improve correlations made with the anatomical distribution of NMSC incidence data. The measured patterns in UV exposure presented in this research can be applied to a variety of SZA ranges providing a detailed data set of UV exposures that may assist in future studies assessing the anatomical distribution of melanoma and NMSC incidence.

Conclusions

Measurements of body surface UV exposure patterns have been presented with respect to changing SZA. These measurements improve upon previously available data which is often limited to fewer isolated body sites. The presented collection of measured UV exposure data is of further importance in detailing the solar exposures that affect human skin surfaces which are influenced by shading caused by the body itself and surface orientation with respect to the diffuse skylight and the direct solar beam. A total of 2491 measurements of ER to the face, neck, forearm, hand and leg have confirmed that exposures received by the face and back of the neck are greater than exposures received by both the upper and lower limbs. Of each of the studied body parts, the anatomical distribution of BCC and SCC is greatest to the face and upper limbs, particularly the dorsum of the hand and forearm[15,16,17,26]. Incidence rates of both

types of NMSC are particularly high at the nose[14,15] and correlate with the facial ER measurements taken in this research across all SZA ranges.

Acknowledgements

The authors would like to offer their sincere thanks to Professor Bruce Armstrong, School of Public Health, University of Sydney and Dr Georgina Long, Sydney Melanoma Unit, for their assistance in this research. One of the authors, Nathan Downs, received funding through an Australian postgraduate award scholarship.

References

1. T.L. Diepgen and V. Mahler, The epidemiology of skin cancer, *Br. J. Dermatol.*, 2002, **146**(s61), 1-6.

2. E. Konishi and Y. Yoshizawa, Estimation of depth of basal cell layer of skin for radiation protection, *Radiat. Prot. Dosimet.*, 1985, **11**(1), 29-33.

3. B.A. Raasch, P.G. Buettner and C.Garbe, Basel cell carcinoma: histological classification and body-site distribution, *Br. J. Dermatol*. **155**, 401-407.

4. M.P. Staples, M. Elwood, R.C. Burton, J.L. Williams, R. Marks and G.G. Giles, Non-melanoma skin cancer in Australia: the 2002 national survey and trends since 1985, *Med. J. Aust.*, 2006, **184**, 6-10.

5. F.R. deGruijl, Skin cancer and solar UV radiation, *Eur. J. Cancer*, 1999, **35**(14), 2003-2009.

6. J.A. Parrish, K.F. Jaenicke and R.R. Anderson, Erythema and melanogenesis action spectra of normal human skin, *Photochem. Photobiol.* 1982, **36**, 187-191.

7. M. Staples, R. Marks and G. Giles, Trends in the incidence of non-melanocytic skin cancer (NMSC) treated in Australia 1985-1995: Are primary prevention programs starting to have an effect? *Int. J. Cancer*, 1999, **78**(2), 144-148 .

8. R. Marks, G. Rennie and T. Selwood, The relationship of basal cell carcinomas and squamous cell carcinomas to solar keratoses, *Arch. Dermatol.*, 1988, **124**(7), 1039-1042.

9. C.A. Frost and A.C. Green, Epidemiology of soalr keratoses, *Br. J. Detmatol*., 1994, **131**(4), 455-464.

10. R.Marks, D. Rennie and T.S. Selwood, Malignant transformation of solar keratosse to squamous cell carcinoma, *Lancet*, 1988, **1**(8589), 795-797.

11. J. Röwert-Huber, M.J. Patel, T. Forschner, C.Ulrich, J.Eberle, H. Kerl, W. Sterry and E. Stockfleth, Actinic keratosis is an early in situ squamous cell carcinoma: a proposal for reclassification, *Br. J. Dermatol*., **156**, 8-12.

12. T.D. Nguyen, V. Siskind, L. Green, C. Frost and A. Green, Ultraviolet radiation, melanocytic naevi and their dose-response relationship, *Br. J. Dermatol.*, 1998, **137**, 91-95.

13. B.L. Diffey, T.J. Tate and A. Davis, Solar dosimetry of the face: the relationship of natural ultraviolet radiation exposure to basal cell carcinoma localisation, *Phys. Med. Biol.*, 1979, **24**, 931-939.

14. R.H. Brodkin, A.W. Kopf and R. Andrade, Basal-cell epithelioma and elastosis: a comparison of distribution, in *The Biologic Effects of Ultraviolet Radiation: with Emphasis on the Skin*, ed. F. Urbach, Pergamon, New York, 1969, pp. 581-618.

15. D.K. Pearl and E.L. Scott, The anatomical distribution of skin cancers, *Int. J. Epidemiol.*, 1986, **15**(4), 502-506.

16. A. Kricker, D.R. English, P.L. Randell, P.J. Heenan, C.D. Clay, T.A. Delaney and B.K. Armstrong, Skin cancer in Geraldton, Western Australia: a survey of incidence and prevalence, *Med. J. Aust.*, 1990, **152**(8), 399-407.

17. B. Raasch, R. Maclennan, I. Wronski and I. Robertson, Body site specific incidence of basal and squamous cell carcinoma in an exposed population, Townsville, Australia, *Mutat. Res. Fundam. Mol. Mech. Mugag.*, 1998, **422,** 101-106.

18. N.J. Downs and A.V. Parisi, Three dimensional visualisation of human facial exposure to solar ultraviolet, *Photochem. Photobiol. Sci.*, 2007, **6,** 90-98.

19. B.L. Diffey, Ultraviolet radiation dosimetery with polysulphone film, in *Radiation Measurement in Photobiology* ed. B.L. Diffey, Academic Press, London, 1989, pp. 135-159.

20. A. Green, D. Battistutta, V. Hart, D. Leslie, G. Marks, G. Williams, P. Gaffney, P. Parsons, L. Hirst, C. Frost, E. Orrell, K. Durham and C. Lang, The Nambour skin cancer and actinic eye disease prevention trial: design and baseline characteristics of participants, *Controlled Clin. Trials*, 1994, **16**, 512-522.

21. F. Urbach, Environmental risk factors for skin cancer, *Recent Results Cancer Res*., 1993, **128**, 243-262.

22. M.G. Kimlin, A.V. Parisi and J.C.F. Wong, The facial distribution of erythemal ultraviolet exposure in south east Queensland, *Phys. Med. Biol.*, 1998, **43,** 231-240.

23. N.J. Downs, M.G. Kimlin, A.V. Parisi and J.J. McGrath, Modelling human facial UV exposure, *Radiat. Prot. Aust.*, 2001, **17**(3), 103-109.

24. Y. Scrivener, E. Grosshans and B. Cribier, Variation of basal cell carcinomas according to gender, age, location and histopathological subtype, *Br. J. Dermatol.*, 2002, **147,** 41-47.

25. N.M. Richmond-Sinclair, N. Pandeya, R.S. Ware, R.E. Neal, G.M. Williams, J.C., van der Pols and A.C Green, Incidence of basal cell carcinoma multiplicity and detailed anatomic distribution: longitudinal study of an Australian population, *J. Invest., Dermatol.*, 2009, **129**(2), 323-328.

26. G.G. Giles, R. Marks and P. Foley, Incidence of non-melanocytic skin cancer treated in Australia, *Br. Med. J.*, 1988, **296**(6614), 13–17.

Supplementary Information: Tables

Sup Table 1(a). Facial site exposure ratio measured between 2005 and 2008 and expressed as a percentage for the SZA range 0^{o}-30^{o}. ER ranges in the table show high exposed areas in red (ER: 75-100), mid exposed areas in blue (ER:25-74) and low exposed areas uncloured (ER: 0-25).

	Cv1	Cv2	Cv3	Cv4	Cv5	Cv6	Cv7	Cv8	Cv9	Cv10	Cv11	Cv12	Cv13	Cv14	Cv15	Cv16	Cv17	Cv18
	100	100	82	85	77	96												
Ch1	67	100	84	95	95		85	58										
Ch2		100	80	77	85		64		70	86								
Ch3	87	80	84		76		88	68	71	81	72							
Ch4		78	74		89				46	94	74	69						
Ch5					56		79			41		79	65					
Ch6		70	53								28		40	55				
Ch7					49			56	49	67		46		53				
Ch8		38	58										38	48	42			
Ch9					58		45			62	42				47			
Ch10		51	52		50				54					36	29			
Ch11					88			84		45				45		36		
Ch12		30	45				49				29	33	29	27	29	26		
Ch13					50				54	69					46	40		
Ch14		56	34						69	60		29			22	17		
Ch15					51		42			43		48		25		22		
Ch16		32	27						4			23	35		13	23		
Ch17					4					7		14		22	29	18		
Ch18		17	6		8		10							27	17	22		
Ch19					8					16	9	9	15	26				
Ch20	59	23	11		7									25	19	19		
Ch21					7			15		21	8	8		25	14		65	
Ch22	70	55	42		17										18	31	75	
Ch23	59	40	32			31		35		31	40	21	29	25	21			
Ch24		55	34		54			34		40				17		19	22	31
Ch25	27	19	47		44			48			47	34	22					
Ch26				40						29				26	20	7	13	25
Ch27		5	8		30			35			29	18	24	14	28			9
Ch28					25					24				16	12	20	26	
Ch29		12	19					27			17	9	14	15			8	
Ch30	28		37		38		36		19	15	14	12	17	15		20		
Ch31		40	46					26			10	9		15		17		
Ch32					33					20		13		8		10		
Ch33		5	8					21			14	12	13	6				
Ch34					26					19		16						
Ch35		25	28					14			18	15	15					
Ch36					16	12				21								
Ch37		7	7					26	16		19	14						
Ch38					19		27	19		18		10						
Ch39		33	29								12	13						
Ch40					38			19		15	7							
Ch41		21	16						11	5		19						
Ch42					6	10	8	7	3	11								
Ch43		4	5			4	3	8				25						
Ch44	1	1	1		3		5			23								
Ch45			3	2								28						
Ch46					7		9	15		18								
Ch47			7									29						
Ch48					13		14			17								
Ch49			9		11			18				29						

Sup Table 1(b). Facial site exposure ratio measured between 2005 and 2008 and expressed as a percentage for the SZA range 30°-50°. ER ranges in the table show high exposed areas in red (ER: 75-100), mid exposed areas in blue (ER:25-74) and low exposed areas uncloured (ER: 0-25).

	Cv1	Cv2	Cv3	Cv4	Cv5	Cv6	Cv7	Cv8	Cv9	Cv10	Cv11	Cv12	Cv13	Cv14	Cv15	Cv16	Cv17	Cv18
			69															
Ch1	100		97					70										
Ch2							100											
Ch3			69					63										
Ch4							100											
Ch5	71	66		70		70		64		75	66	75	57					
Ch6			61				90											
Ch7	65												56	88				
Ch8			45				79	55										
Ch9	62													70	46			
Ch10							58						10					
Ch11	66							60						53	46			
Ch12							77											
Ch13	69												32	51				
Ch14		16		48		54	82	57		59		47	33	29	33	32		
Ch15	66							49						40				
Ch16							12						37		32			
Ch17	35													42				
Ch18							13	9										
Ch19	38												26	48				
Ch20							21	16										
Ch21	82		27											42				
Ch22							33						44					
Ch23	98		46					37						60				
Ch24		47		53		57	83	58		58		52	43	36	28		20	24
Ch25	56		36					49					38	47	17			
Ch26							51											
Ch27	9													32	31			
Ch28			16				39	34										
Ch29	31												22	32				
Ch30							54								30			
Ch31	67	44	35	45		39		30		19		18	20	25		20		
Ch32							40						21					
Ch33	12		8											6				
Ch34							31	24					15					
Ch35	50		37															
Ch36							26						18					
Ch37	11							19										
Ch38			18				42											
Ch39	54							21										
Ch40			35				38											
Ch41	34	16		16		41		14										
Ch42			17					8										
Ch43	8																	
Ch44							13	11										
Ch45																		
Ch46	8						24	21										
Ch47																		
Ch48	12						25											
Ch49								26										

Sup Table 1(c). Facial site exposure ratio measured between 2005 and 2008 and expressed as a percentage for the SZA range 50^{o}-80^{o}. ER ranges in the table show high exposed areas in red (ER: 75-100), mid exposed areas in blue (ER:25-74) and low exposed areas uncloured (ER: 0-25).

	Cv1	Cv2	Cv3	Cv4	Cv5	Cv6	Cv7	Cv8	Cv9	Cv10	Cv11	Cv12	Cv13	Cv14	Cv15	Cv16	Cv17	Cv18
	100	100	81	83	100													
Ch1		100		100			73	74										
Ch2	100	96							100									
Ch3							100		79									
Ch4	100	94									63	77						
Ch5							84		92			88	97					
Ch6	78	73												83				
Ch7							80		94				72	72				
Ch8	94	73									66		78	63				
Ch9							90		86									
Ch10	88	78						39					62	100	66			
Ch11							75		79		74					68		
Ch12	88	65						55						61				
Ch13							83		66		60		56			61		
Ch14	92	77						54					52	53	53			
Ch15							82		77							54		
Ch16	56	58						18				53	45	34		57		
Ch17							11		28					43		26		
Ch18	41	29											45	94	31			
Ch19							34		39	18			54			36		
Ch20	67	61											11	43				
Ch21							42	25	39						23	52		
Ch22	100	53	30							38		58		77				
Ch23							59							49	49			65
Ch24	33	75						83	64			83	52	44		31		
Ch25			46				79	51			82						16	47
Ch26	25	26							73					47				
Ch27							56	37					51		49			37
Ch28	21	15									47	23		51				
Ch29							52		51				22		34		25	
Ch30	65	63						40			33			30				
Ch31							59						28	27		37		
Ch32	39	39						56	44		33	33		34				
Ch33							45						24	8				
Ch34	64	72									22							
Ch35							39	39	30			38	41					
Ch36	22										45							
Ch37		15					41	37										
Ch38	36								35		36	29						
Ch39		66				45	63					23						
Ch40	62							24			18	44						
Ch41		33				43	25		22			38						
Ch42	29																	
Ch43		10					8		28	43		36						
Ch44	7	0																
Ch45	1	1					14		40	35		27						
Ch46																		
Ch47	13						15			46		58						
Ch48									52									
Ch49	28	16					35			33		43						

Sup Table 2(a). Site exposure ratio measured to the back of the neck and expressed as a percentage for the SZA range 0^{o}-30^{o} and cloud cover less than 4 oktas measured between 2005 and 2008. ER ranges in the table show high exposed areas in red (ER: 75-100), mid exposed areas in blue (ER:25-74) and low exposed areas uncloured (ER: 0-25).

	Cv1	Cv2	Cv3	Cv4	Cv5	Cv6	Cv7	Cv8	Cv9
Ch1	6		6	17	7	16	8		
Ch2	10		9		12		12		
Ch3	13		14		14		12		
Ch4	14		18		17		15		
Ch5	20		15	20	20	24	19		
Ch6	19		17		21	23	19		
Ch7	20		18		17	26	23		
Ch8	21		22		23	34	27		
Ch9	17		22	28	21	18	32		
Ch10	20		22		29		32	50	
Ch11	23		23		32		37	52	50
Ch12	19		20		26		30	38	48
Ch13	24		28		20	39	34	36	40

Sup Table 2(b). Site exposure ratio measured to the back of the neck and expressed as a percentage for the SZA range 30^{o}-50^{o} and cloud cover greater than 4 oktas measured between 2005 and 2008. ER ranges in the table show high exposed areas in red (ER: 75-100), mid exposed areas in blue (ER:25-74) and low exposed areas uncloured (ER: 0-25).

	Cv1	Cv2	Cv3	Cv4	Cv5	Cv6	Cv7	Cv8	Cv9
Ch1		14		13		13			
Ch2		21		21		16			
Ch3		24		23		23			
Ch4		32		30		27			
Ch5		38		35		32			
Ch6		33		37		35			
Ch7		56		33		35			
Ch8		35		32		47			
Ch9		37		38		44			
Ch10		33		44		44		62	
Ch11		40		30		40		49	53
Ch12		43		69		42		59	
Ch13		38		42		44		48	

Sup Table 2(c). Site exposure ratio measured to the back of the neck and expressed as a percentage for the SZA range 50^{o}-80^{o} and cloud cover less than 4 oktas measured between 2005 and 2008. ER ranges in the table show high exposed areas in red (ER: 75-100), mid exposed areas in blue (ER:25-74) and low exposed areas uncloured (ER: 0-25).

	Cv1	Cv2	Cv3	Cv4	Cv5	Cv6	Cv7	Cv8	Cv9
Ch1	19								
Ch2									
Ch3	43								
Ch4									
Ch5	49				47		48		
Ch6			49						
Ch7	59				62		57		
Ch8			48						
Ch9	58				66		69		
Ch10			56						
Ch11	45				63		77		86
Ch12			60						
Ch13	62				68		68		73

Sup Table 3(a). Site exposure ratio measured to the arm and expressed as a percentage for the SZA range 0^{o}-30^{o} and cloud cover less than 4 oktas measured between 2005 and 2008. ER ranges in the table show high exposed areas in red (ER: 75-100), mid exposed areas in blue (ER:25-74) and low exposed areas uncloured (ER: 0-25). Contours located on the anterior of the arm recorded the highest exposures.

	Cv1	Cv2	Cv3	Cv4	Cv5	Cv6	Cv7	Cv8	Cv9	Cv10	Cv11	Cv12	Cv13	Cv14	Cv15	Cv20	Cv21	Cv22	Cv23
Ch1																			
Ch2																			
Ch3																			
Ch4																			
Ch5																			
Ch6																			
Ch7																			
Ch8																			
Ch9																			
Ch10																			
Ch11																			
Ch12																			
Ch13																		5	9
Ch14	18	9	6	7	21	5	20	15		8								8	13
Ch15	25	43	43	31	54	23	35	31	13	17	13					3	4	9	10
Ch16	13	23	38	39	61	49	37	32	20	23	17				3		3	6	7
Ch17	12	19	29	30	54	60	40		27	21	19	8	4	3					7
Ch18	8	13	19	27	38	36	44	42	23	22	13	13			3			5	6
Ch19	6	10	19	29	31	40	43	36	25	23		11	8	5			3	5	
Ch20	5	9	13	23	30	41	39					10	6	4	4				
Ch21				18	29	43			40				6	3	4				
Ch22						35							5	4	4				
Ch23						27							5		6				
Ch24													7	3	4				
Ch25															3				
Ch26														4					
Ch27													8		3				
Ch28														4					

Sup Table 3(b). Site exposure ratio measured to the arm and expressed as a percentage for the SZA range 30°-50° and cloud cover less than 4 oktas measured between 2005 and 2008. ER ranges in the table show high exposed areas in red (ER: 75-100), mid exposed areas in blue (ER:25-74) and low exposed areas uncloured (ER: 0-25). Measurements made underneath the shirt covering the shoulder had an ER of 0. Contours located on the anterior of the arm recorded the highest exposures.

	Cv1	Cv2	Cv3	Cv4	Cv5	Cv6	Cv7	Cv8	Cv9	Cv10	Cv11	Cv12	Cv13	Cv14	Cv15	Cv20	Cv21	Cv22	Cv23
Ch1																			
Ch2					0														
Ch3							0			0									
Ch4												0							
Ch5					0		0												
Ch6	0									0					0				
Ch7					0														
Ch8										0		0				0		0	
Ch9	0		0		0		0												
Ch10								0	0					0				0	
Ch11	0		0		0	0						0				0			
Ch12							9		1									3	1
Ch13	10	0	1	1	7		14	8	7	4				0				8	13
Ch14	18	1	20	8	38	5	13	24	11	6	5	0					6		14
Ch15	22	28	30	44	49	31	39	40	25	25	17	5		2	3	0	7	15	10
Ch16	18	25	29	51	46	47	45	46	29	28	25	9	5		4			8	9
Ch17	17	23	19	40	43	33	49	43	36	32	20			3	4		6	6	8
Ch18	7	17	33	41	45	45	37	35	34	22	17	22	11					2	8
Ch19	8	20	29	33	48	49	37	55	41	28		16	13	7	3		6	7	
Ch20	4		20	24	42	42	45		17			14	10	5					
Ch21				23	39	47	19		38				9	5	6				
Ch22						39							7	3					
Ch23						30									7				
Ch24															6				
Ch25													11	4					
Ch26																			
Ch27													11	4	5				
Ch28													15						

Sup Table 3(c). Site exposure ratio measured to the arm and expressed as a percentage for the SZA range 50°-80° and cloud cover less than 4 oktas measured between 2005 and 2008. ER ranges in the table show high exposed areas in red (ER: 75-100), mid exposed areas in blue (ER:25-74) and low exposed areas uncloured (ER: 0-25). Contours located on the anterior of the arm recorded the highest exposures.

	Cv1	Cv2	Cv3	Cv4	Cv5	Cv6	Cv7	Cv8	Cv9	Cv10	Cv11	Cv12	Cv13	Cv14	Cv15	Cv20	Cv21	Cv22	Cv23
Ch1																			
Ch2																			
Ch3																			
Ch4																			
Ch5																			
Ch6																			
Ch7																			
Ch8																			
Ch9																			
Ch10																			
Ch11														2					
Ch12								11											20
Ch13						6				25					4				24
Ch14	27	20	39	31			66	64	43		46		13						23
Ch15	32	27				61		71		49	65				13	12		14	
Ch16		41	47	62	67			87	76	66	49		23						
Ch17	19	26		55	51	58	72	61	63	54		24		16				11	19
Ch18	19	23	41	55	54		71	69		60	49	41	37		13				
Ch19	12	14	32	47	52	60	63	82	57	44		43		26					
Ch20	11	22		36		55	58	56	66			48	29	18					
Ch21				29	43	54	65						30						
Ch22													19	12					
Ch23						45													
Ch24														12					
Ch25													29						
Ch26														20					
Ch27																			
Ch28													46	21					

Sup Table 4(a). Site exposure ratio measured to the hand and expressed as a percentage for the SZA range 0^{o}-30^{o} and cloud cover less than 4 oktas measured between 2005 and 2008. ER ranges in the table show high exposed areas in red (ER: 75-100), mid exposed areas in blue (ER:25-74) and low exposed areas uncloured (ER: 0-25). The dorsa of the hand received the highest exposures. For this research the mannequin hand was titlted from the arm's longitudinal axis increasing the UV radiation received due to the increased proportion of the hand oriented toward a horizontal plane.

	Cv1	Cv2	Cv3	Cv4	Cv5	Cv6	Cv7	Cv8	Cv9	C10	C11	C12	C13	C14	C15	C16	C17	C18	C19	C20	C21	C22	C23
Ch1																	4			4			
Ch2						22													4				
Ch3							42									8		3			13		
Ch4					11	31	45									6			3				
Ch5					37	49	48	37	35	30	27					7			3		14		
Ch6						65		35	34	24	15					5							
Ch7					52	76		62		44	26					2							
Ch8				20	69			52		46	30	11				2					3		
Ch9			16		76	73		73		50	42	34		2	5							5	
C10		29		57	66	75		72		48	52	53	6	2	2		1			2		3	10
C11		42	69	51	57	75		71		61	56	53				1				2	1		6
C12			31	63	47	65		63		56		38						2				1	6
C13	32		29	10	42		33	70		40		23				3			2				3
C14		26	22		37	67	9	62		61	8				2			5		8			
C15			17		30	65			10							5							
C16					41	54	3	58		29	28							8	3				
C17					37	17		41		14													
C18					46			11		7													
C19					41			11		9													
C20								9															

Sup Table 4(b). Site exposure ratio measured to the hand and expressed as a percentage for the SZA range 30^{o}-50^{o} and cloud cover less than 4 oktas measured between 2005 and 2008. ER ranges in the table show high exposed areas in red (ER: 75-100), mid exposed areas in blue (ER:25-74) and low exposed areas uncloured (ER: 0-25). The dorsa of the hand received the highest exposures. For this research the mannequin hand was titlted from the arm's longitudinal axis increasing the UV radiation received due to the increased proportion of the hand oriented toward a horizontal plane.

	Cv1	Cv2	Cv3	Cv4	Cv5	Cv6	Cv7	Cv8	Cv9	C10	C11	C12	C13	C14	C15	C16	C17	C18	C19	C20	C21	C22	C23
Ch1																		6			15		
Ch2						31										12			6				
Ch3																		5		12	20		
Ch4					21	46	57									10	5				22		
Ch5					50			45	42	44	33							5					
Ch6					61	62	70	53	45		18								6				
Ch7					64	74			56		32					5	4			6			
Ch8				35				61	55	53	41	25	10		20			2					
Ch9			34		52	76	70	70		58		34		3	7	2		1				10	
C10		47		61	67	66			58		52								3		3		20
C11			66					71		51	53	58				3		3					13
C12	39		64	67	53	70	60	46	53	56				4						11		5	
C13		69	31	10			37			51	32	33											9
C14		47			52	72		60	10							8				15			
C15			16		48	68				60					4			17					
C16						60	15	61	11														
C17					51	31		45		20													
C18					60			24															
C19					57			15		14													
C20								15															

Sup Table 4(c). Site exposure ratio measured to the hand and expressed as a percentage for the SZA range 50°-80° and cloud cover greater than 4 oktas measured between 2005 and 2008. ER ranges in the table show high exposed areas in red (ER: 75-100), mid exposed areas in blue (ER:25-74) and low exposed areas uncloured (ER: 0-25). The dorsa of the hand received the highest exposures. For this research the mannequin hand was titlted from the arm's longitudinal axis increasing the UV radiation received due to the increased proportion of the hand oriented toward a horizontal plane.

	Cv1	Cv2	Cv3	Cv4	Cv5	Cv6	Cv7	Cv8	Cv9	C10	C11	C12	C13	C14	C15	C16	C17	C18	C19	C20	C21	C22	C23
Ch1																							
Ch2																			3				
Ch3						60											3						
Ch4							60									17			7		39		
Ch5					58		71		60		41												
Ch6						57			53		27						7		10				
Ch7								71		45											0		
Ch8					53	84				68		35	17		17	0		0					
Ch9						75		80		58				0			0		0		3		
C10				58		73		42		59					0		0		0				41
C11			67			60		66		56				5		2				6			
C12				70	52	58		78		63													20
C13				10		68		62		53		34								20			
C14		42	31		40	72	7	77								15		12					
C15						60		73		60													
C16					76	67	20																
C17						34		61										26					
C18					65					8													
C19								36															
C20																							

Sup Table 5(a). Site exposure ratio measured to the leg and expressed as a percentage for the SZA range 0^{o}-30^{o} and cloud cover less than 4 oktas measured between 2005 and 2008. ER ranges in the table show high exposed areas in red (ER: 75-100), mid exposed areas in blue (ER:25-74) and low exposed areas uncloured (ER: 0-25). No exposures were measured to contours Cv0, Cv1 or Cv2 as these were protected by the mannequin's shorts which were worn during the measurement period.

	Cv3	Cv4	Cv5	Cv6	Cv7	Cv8	Cv9	Cv10	Cv11	Cv12	Cv13	Cv14	Cv15
Ch1						7	6	9					
Ch2						6	6	22					
Ch3					1	9	5						
Ch4		0	0	1	3	10	5		0	0	0	0	0
Ch5	0	3	2	2	4	11				0	0	0	0
Ch6	1	6	4	4	5	10			0	0	0	0	0
Ch7	6	8	8	6	8	9			7	12	13	9	1
Ch8		11	12	10	11	9			10	13	16	13	7
Ch9		13	15	14	15	10			10	10	15	12	9
Ch10		15	19	17	18	9			8	8	11	11	19
Ch11		14	19	19	19	10			8	6	7	11	17
Ch12		20	23	19	16	7			7	6	6	13	15
Ch13		23	20	21	16	12			6	8	8	15	15
Ch14		21	21	20	14	12			7	7	9	16	13
Ch15		20	20	19	14	14			9	8	9	14	16
Ch16		20	19	18	14	13			9	8	9	13	
Ch17			16	16	14	16			11	10	9	12	
Ch18			16	18	15	17			9	9	9	12	
Ch19			15	15	15	24			8	10	9	11	
Ch20			13	15	15				7	8	9	10	
Ch21			15	16	17				6	10	9	8	
Ch22				16	17				7	9	10	11	
Ch23				17	16				7	9	10	11	
Ch24				18	17				6	10	9	12	
Ch25				14	16				8	9	10	13	
Ch26				14	19				8	10	11	14	
Ch27					24				8	11	10	13	
Ch28					16				7	11	11	12	
Ch29									9	10	12		
Ch30									10	10	12		
Ch31									10	11	16		
Ch32									9	10	13		
Ch33										10	12		

Sup Table 5(b). Site exposure ratio measured to the leg and expressed as a percentage for the SZA range 30°-50° and cloud cover less than 4 oktas measured between 2005 and 2008. ER ranges in the table show high exposed areas in red (ER: 75-100), mid exposed areas in blue (ER:25-74) and low exposed areas uncloured (ER: 0-25). No exposures were measured to contours Cv0, Cv1 or Cv2 as these were protected by the mannequin's shorts which were worn during the measurement period.

	Cv3	Cv4	Cv5	Cv6	Cv7	Cv8	Cv9	Cv10	Cv11	Cv12	Cv13	Cv14	Cv15
Ch1						17	13	18					
Ch2					4	21	11	35					
Ch3		4	5	6	9	23	11						
Ch4	6	11	9	8	12	25	10						
Ch5	13	15	13	13	13	31			14	20	17		9
Ch6	21	22	18	15	20	25			16	22	25	37	19
Ch7	25	28	29	21	25	21			17	22	28	38	30
Ch8		34	33	18	38	22			17	20	26	22	29
Ch9		37	34	29	43	23			14	17	25	44	30
Ch10		52	29	38	38	23			14	10	24	44	42
Ch11		43	45	31	42	22			11	12	22	42	45
Ch12		44	44	38	33	27			13	13	21	43	31
Ch13		37	47	36	33	28			10	13	21	48	35
Ch14		33	39	44	36	35			12	12	21	46	33
Ch15		39	32	28	33	30			18	15	21	40	33
Ch16		36	32	32	30	40			14	14	21	36	
Ch17			27	31	34	35			14	14	21	35	
Ch18			29	35	35	46			14	14	20	22	
Ch19			34	31	45	41			13	14	15	26	
Ch20			21	28	41				12	13	16	27	
Ch21			32	38	48				11	15	16	26	
Ch22				38	39				11	14	17	23	
Ch23				32	36				14	16	18	29	
Ch24				26	36				11	15	19	32	
Ch25				33	37				13	15	24	29	
Ch26				26	39				16	16	19	33	
Ch27					43				13	18	23	26	
Ch28					44				15	17	25	25	
Ch29									15	18	23		
Ch30									16	19	23		
Ch31									14	21	22		
Ch32									15	19	28		
Ch33										14	25		

Sup Table 5(c). Site exposure ratio measured to the leg and expressed as a percentage for the SZA range 50°-80° and cloud cover less than 4 oktas measured between 2005 and 2008. ER ranges in the table show high exposed areas in red (ER: 75-100), mid exposed areas in blue (ER:25-74) and low exposed areas uncloured (ER: 0-25). No exposures were measured to contours Cv0, Cv1 or Cv2 as these were protected by the mannequin's shorts which were worn during the measurement period.

	Cv3	Cv4	Cv5	Cv6	Cv7	Cv8	Cv9	Cv10	Cv11	Cv12	Cv13	Cv14	Cv15
Ch1						33	24						
Ch2					12								
Ch3					19	36							
Ch4					22								
Ch5		35		35							47		
Ch6	43		42		40								
Ch7	50		38	36					32		50	36	51
Ch8		45	15		58								38
Ch9		63	70	41					34	37	51	56	
Ch10		62	42	58	65						37		77
Ch11		64	62	65	55				24	25		40	
Ch12		71	70		52						31		48
Ch13		62	75		46				27	25			
Ch14		60	53		56						35		47
Ch15		43	59	59	40				39	25		61	52
Ch16		62	60		45						27		
Ch17			53		44					27		57	
Ch18			56	59	51						41		
Ch19			55		57					33		42	
Ch20			46	51							45		
Ch21			49		57					24			
Ch22				58							32		
Ch23				54	60					33		37	
Ch24				51							26		
Ch25				52	58							53	
Ch26				51	53						42		
Ch27					61							45	
Ch28					50						49		
Ch29													
Ch30											41		
Ch31													
Ch32											40		
Ch33													

Supplementary Information: Figures

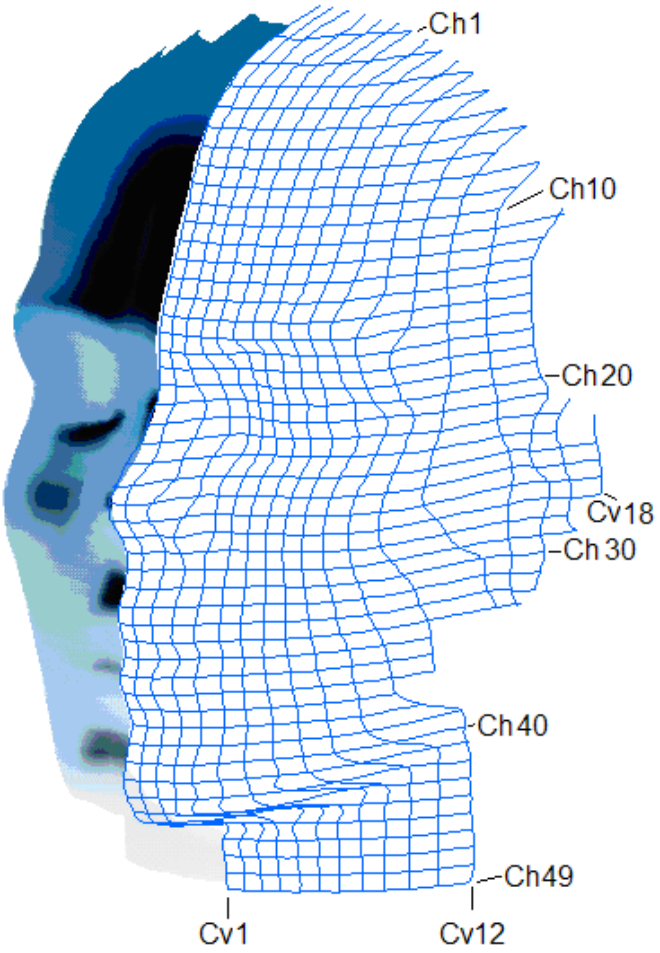

Sup Figure 1. Horizontal (Ch) and vertical (Cv) facial contour assignments.

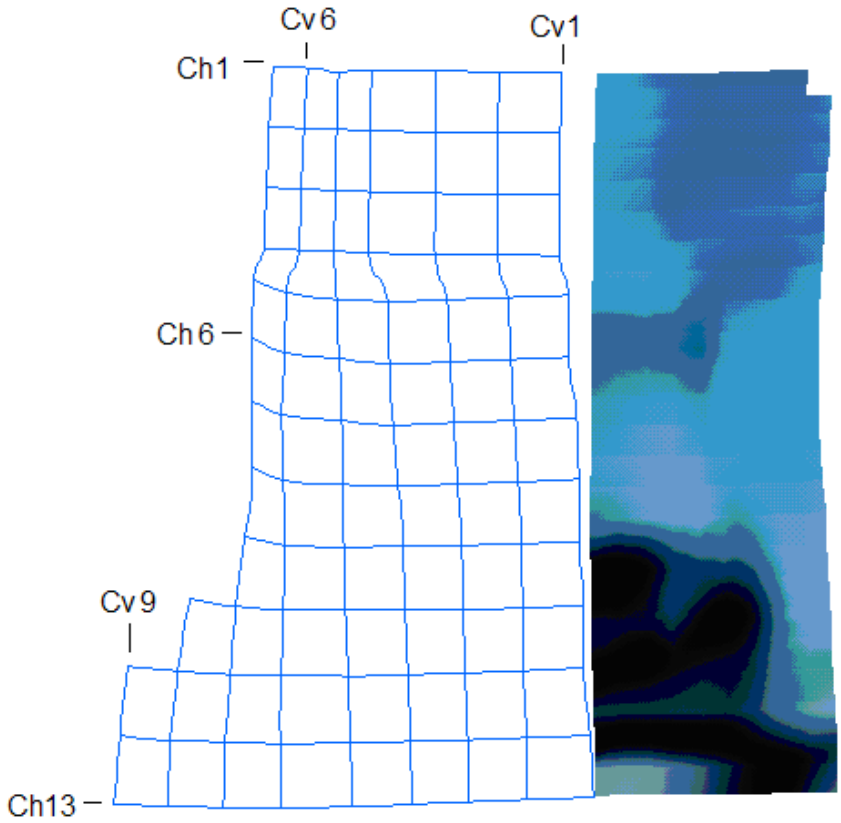

Sup Figure 2. Horizontal (Ch) and vertical (Cv) neck contour assignments.

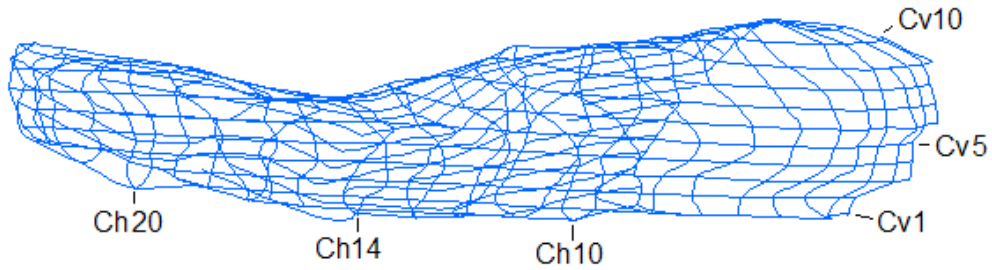

Sup Figure 3. View of three dimensional arm surface from behind the shoulder. Contours marked Cv1 through Cv23 are oriented along the arm's longitudinal axis. Anterior contours Cv1, Cv5 and Cv10 are shown. Contours marked Ch10, Ch14 and Ch20 are also shown on the diagram. These contours formed complete bands around the arm surface and were numbered from the shoulder (figure right) to the wrist (figure left). Vertical and horizontal contour assignments were given for the arm in its natural position when attached to the body mannequin such that banded contours are the horizontal contours in the wireframe.

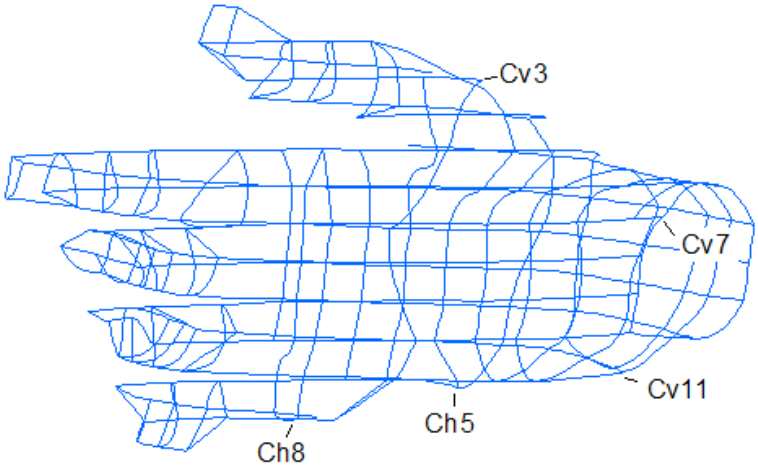

Sup Figure 4. Contours marked Cv1 through Cv23 represent the longitudinal contours extending from the wrist to the finger tips of the three dimensional hand surface. These contours start and end on the thumb. Contours banded about the hand surface and individual fingers start from the wrist and extend to the finger tip bands. Contours Ch5 and Ch8 are shown in the figure. Vertical and horizontal contour assignments were given for the hand in its natural position when attached to the body mannequin such that banded contours are the horizontal contours in the wireframe.

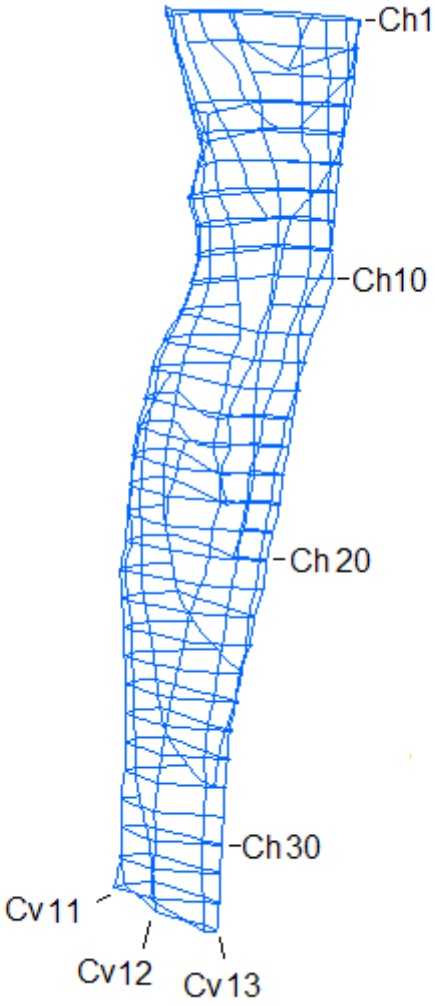

Sup Figure 5. Longitudinal leg contours extending from the upper thigh to the ankle start at Cv0 and end at Cv16. Contours Cv11 through Cv13 are shown in the figure for a forward facing view of the leg model showing the knee positioned to the upper right. Banded contours Ch1, Ch10, Ch20 and Ch30 show the thigh to ankle order in which these contours were labeled.

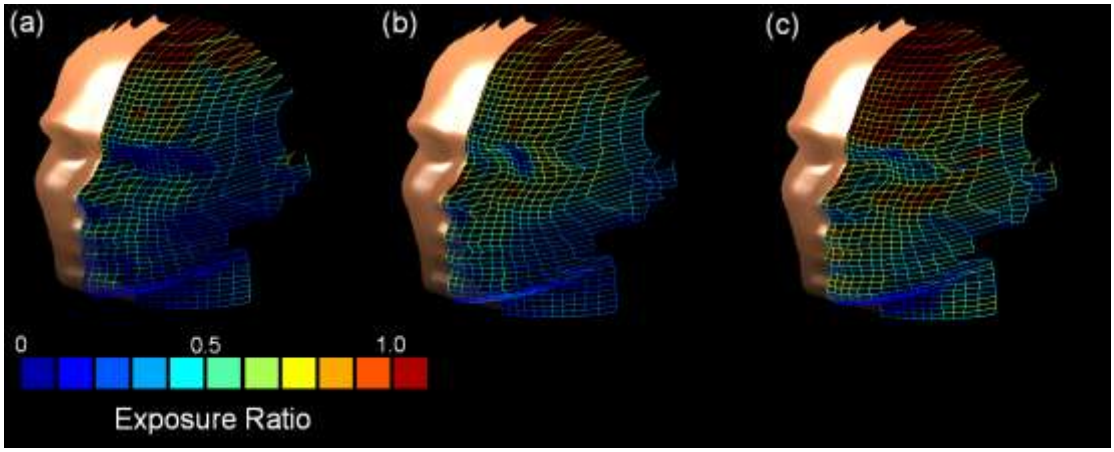

Sup Figure 6. Facial ER measured under low cloud cover conditions over the 2005 to 2008 period. (a) Facial ER measured in the SZA range 0^{o}-30^{o}; (b) Facial ER measured in the SZA range 30^{o}-50^{o}; (c) Facial ER measured in the SZA range 50^{o}-80^{o}.

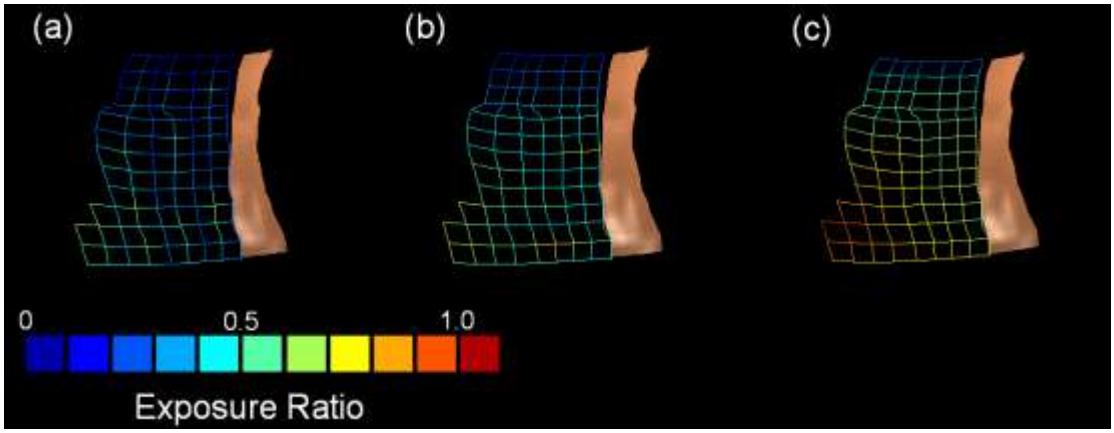

Sup Figure 7. ER measured to the back of the neck under low cloud cover conditions for SZA ranges 0^{o}-30^{o} and 50^{o}-80^{o} and high cloud cover conditions in the SZA range 30^{o}-50^{o} measured over the 2005 to 2008 period. (a) Neck ER measured in the SZA range 0^{o}-30^{o}; (b) Neck ER measured in the SZA range 30^{o}-50^{o}; (c) Neck ER measured in the SZA range 50^{o}-80^{o}. The greatest exposure was measured on the lower region of the neck toward the shoulder.

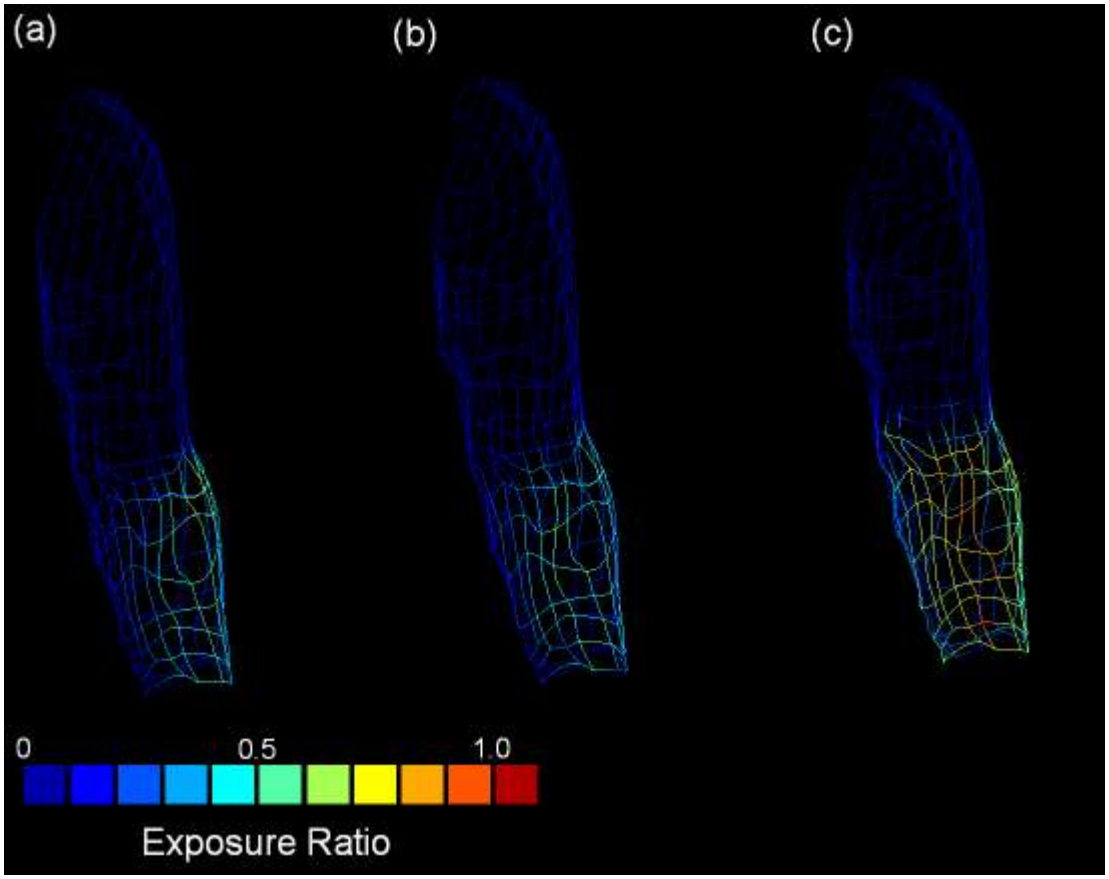

Sup Figure 8. ER measured to the arm under low cloud cover conditions over the 2005 to 2008 period. (a) Arm ER measured in the SZA range 0^{o}-30^{o}; (b) Arm ER measured in the SZA range 30^{o}-50^{o}; (c) Arm ER measured in the SZA range 50^{o}-80^{o}. The anterior region of the lower forearm received the greatest exposure. The shoulder of the mannequin arm was protected by the sleeves of a polo style shirt.

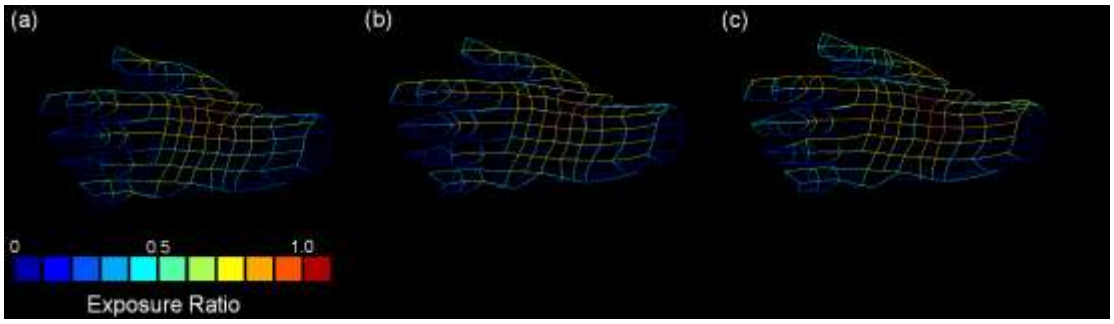

Sup Figure 9. ER measured to the hand under low cloud cover conditions over the 2005 to 2008 period. (a) Hand ER measured in the SZA range 0^{o}-30^{o}; (b) Hand ER measured in the SZA range 30^{o}-50^{o}; (c) Hand ER measured in the SZA range 50^{o}-80^{o}. The palm of the hand received negligible exposures.

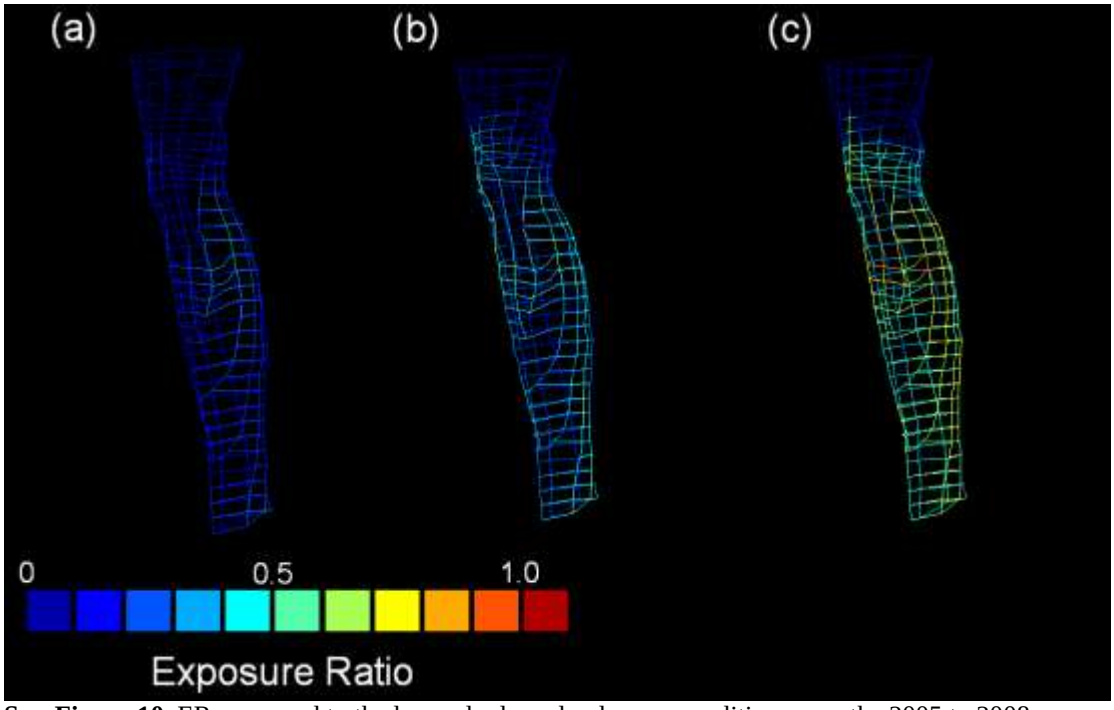

Sup Figure 10. ER measured to the leg under low cloud cover conditions over the 2005 to 2008 period. (a) Leg ER measured in the SZA range 0^{o}-30^{o}; (b) Leg ER measured in the SZA range 30^{o}-50^{o}; (c) Leg ER measured in the SZA range 50^{o}-80^{o}. The greatest exposure was measured over the upper anterior calf muscle region of the mannequin leg.